d-AO Spherical Aromaticity in Ce_6O_8

Xiaohu Yu,*[a] Artem R. Oganov,[a,b,c,d] Ivan A. Popov,[e] and Alexander I. Boldyrev[e]

After the first introduction of π aromaticity in chemistry to explain the bonding, structure, and reactivity of benzene and its derivatives, this concept was further applied to many other compounds featuring other types of aromaticity (i.e., σ, δ). Thus far, there have been no reports on d-AO-based spherical σ aromaticity. Here, we predict a highly stable bare Ce_6O_8 cluster of a spherical shape using evolutionary algorithm USPEX and DFT + U calculations. Natural bond orbital analysis, adaptive natural density partitioning algorithm, electron localization function, and partial charge plots demonstrate that bare Ce_6O_8 cluster exhibits d-AO spherical σ aromaticity, thus explaining its exotic geometry and stability. Ce_6O_8 complex plays an important role in many reactions and is known to exist in many forms, such as in $NH_4[Ce_6(\mu^3O)_5(\mu^3OH)_3(\mu^2\text{-}C_6H_5COO)_9(NO_3)_3(DMF)_3]$*DMF*$H_2O$ compound, which is prepared under room temperature, and acts as an oxidizing agent. © 2015 Wiley Periodicals, Inc.

DOI: 10.1002/jcc.24049

Introduction

Aromaticity in chemistry manifests itself through enhanced stability, low reactivity, bond-length equalization, and high electron detachment energies in photoelectron spectra.[1,2] It was Lipscomb, who extended aromaticity into three-dimensions in 1959.[3] He proposed the term "superaromaticity" to explain the three-dimensional (3D) aromaticity of $B_{12}H_{12}^{2-}$. Explicitly, the idea of 3D aromaticity of deltahedral boranes was put forward by Aihara[4] and by King and Rouvray[5] in 1978. Further advancement of 3D aromaticity was put forward by Kroto et al.[6] who stated "C_{60} appears to be aromatic" based on its prominent intensity in mass spectra. However, careful analysis of aromaticity in C_{60} by Chen et al.[7] revealed that the buckyball is not aromatic in spite of being substantially more thermodynamically stable than neighboring carbon clusters. Later on, it was noticed that fullerenes become more aromatic when they are reduced.[8] In 2000, Hirsch et al.[9,10] proposed a $2(N+1)^2$ rule (N = number of π electrons) for spherical π aromaticity, based on the spherical harmonics of pseudoatoms. In 2011, Poater and Solà.[11] proposed the $2N^2+2N+1$ rule for open-shell spherical aromaticity. Chen and King recently reviewed[12] the introduction of 3D aromaticity in chemistry. At the edge of two centuries, the concept of aromaticity was extended to bare metal clusters[13,14] as well as to metal clusters embedded in bulky protective groups of solid-state materials.[15–18] First 3D aromatic metal cluster Al_6^{2-} was described by Kuznetsov et al.[19] Afterwards, aromaticity concept was further extended to transition metal systems.[20–25] Huang et al.[26] showed the presence of d-orbital σ aromaticity in 4d and 5d transition metal oxide clusters $Mo_3O_9^{2-}$ and $W_3O_9^{2-}$. Subsequently, Zhai et al.[27] found π- and δ-aromaticity in transition metal oxide cluster $Ta_3O_3^-$. Alexandrova and coworkers[28–30] studied aromaticity in transition metal clusters as free systems as well as deposited on the surface and being a part of the surface. Among the transition metals, spherical aromaticity was found in gold clusters,[31] where delocalized bonding is due to the s-AO's of Au. Very recently, Cui et al.[32] reported s-AO-based cubic σ aromaticity in polyzinc compound containing $[Zn_8^I(HL)_4(L)_8]^{12-}$ (L = tetrazole dianion) cluster core. In this article, we predict a structure and explore electronic and thermodynamic properties of a lanthanide oxide cluster Ce_6O_8 featuring the first example of d-AO-based spherical σ aromaticity. As a matter of fact, the synthesis of the $NH_4[Ce_6(\mu^3O)_5(\mu^3OH)_3(\mu^2\text{-}C_6H_5COO)_9(NO_3)_3(DMF)_3]$*DMF*$H_2O$ compound containing Ce_6O_8 core has already been reported.[33] In general, our findings suggest that d-AO spherical aromaticity may exist in many multinuclear transition metal and lanthanide oxide compounds. Chemical bonding analyses reveal that among the valence molecular orbitals (MO) involved in the multicenter metal–metal bonding, there are

[a] X. Yu, A. R. Oganov
Department of Problems of Physics and Energetics, Moscow Institute of Physics and Technology, 9 Institutskiy Land, Dolgoprudny City, Moscow Region 141700, Russia
E-mail: yuxiaohu950203@126.com
[b] A. R. Oganov
Skolkovo Institute of Science and Technology, Skolkovo Innovation Center, 5 Nobel St., Moscow 143026, Russia
[c] A. R. Oganov
Department of Geosciences and Center for Materials by Design, Stony Brook University, Stony Brook, New York 11794
[d] A. R. Oganov
International Center for Materials Discovery, School of Materials Science, Northwestern Polytechnical University, Xi'an, 720072 China
[e] I. A. Popov, A. I. Boldyrev
Department of Chemistry and Biochemistry, Utah State University, Logan, Utah 84322

Author Contributions: X.H.Y. and A.R.O. designed the research. X.H.Y. and I.A.P. performed the calculations. X.H.Y, A.R.O., I.A.P., and A.I.B. interpreted the data and wrote the manuscript.
Competing Financial Interests: The authors declare no competing financial interests.
Contract grant sponsor: Government of the Russian Federation; Contract grant number: 14.A12.31.0003; Contract grant sponsor: National Science Foundation; Contract grant number: CHE-1361413 (to A.I.B.)

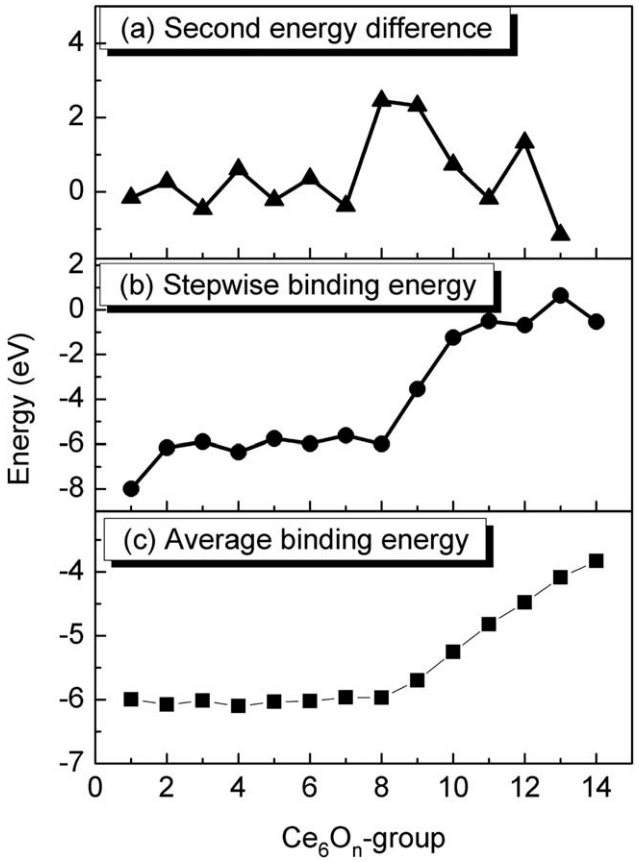

Figure 1. Second energy difference, stepwise and averaged binding energies for global minima of Ce_6O_n ($n = 1$–14) clusters.

two completely delocalized electrons found over six Ce atoms, thus forming the d-AO-based 6c—2e σ bond, which represents a new mode of chemical bonding.

Methods

Searches for stable Ce_6O_n ($n = 1$–14) clusters were performed using the *ab initio* evolutionary algorithm USPEX,[34–36] which has been successfully applied to various materials.[37,38] The first generation of structures was produced using randomly selected point group symmetries and then subsequently relaxed and ranked by the total energy. All the new structures were produced from the old ones by heredity (50%), softmutation (20%), permutation (10%), and 20% of the new generation using the random symmetric algorithm with the target to find the global minimum energy configuration for each composition. In these calculations, we used periodic boundary conditions with vacuum region of 10 Å around each Ce_6O_n cluster.

All structure relaxations and total energy calculations were performed using the Vienna *ab initio* simulation package[39,40] based on density functional theory (DFT) at the GGA level (Perdew-Burke-Ernzerhof functional[41]) with the inclusion of on-site Coulomb interaction ($U_{eff} = U–J = 5$ eV).[42,43] This DFT + U method was chosen as our computational approach due its efficiency and adequacy (on the contrary, standard GGA functionals are not adequate for describing Ce-4f electronic states, which result from the formation of oxygen vacancies in ceria). We used all-electron projector-augmented wave method and plane wave kinetic energy cutoff of 400 eV. $5s^25p^65d^14f^16s^2$ electrons of cerium atoms and $2s^22p^4$ electrons of oxygen atoms were treated as fully relaxed valence electrons. Structure optimizations were performed until the Hellmann–Feynman force on each atom was less than 0.001 eV/Å. Vibrational frequency calculations were performed to check that all stable structures have no imaginary frequencies.

To understand the unique chemical bonding in the bare Ce_6O_8 cluster, we have utilized natural bond orbital analysis (NBO)[44] and its extension adaptive natural density partitioning (AdNDP) method[45] at the UPBE0/Ce/Stuttgart RSC 1997 ECP/O/6-311++G(d,p) level of theory. AdNDP was shown to be a useful tool for deciphering chemical bonding in various clusters[46,47] and solid-state systems.[48,49]

Results and Discussion

We initially performed an extensive search for global minimum structures of all Ce_6O_n ($n = 1$–14) clusters at the DFT + U level of theory. The global minimum structure of bare Ce_6O_8 cluster, which was found to be particularly stable, was then recalculated with higher precision. To find which compositions display particularly high stability, we considered the second energy difference defined as:

$$\Delta^2 E = 2E(Ce_6O_n) - E(Ce_6O_{n-1}) - E(Ce_6O_{n+1}), \quad (1)$$

where $E(Ce_6O_n)$ is the energy of the Ce_6O_n cluster. From the second energy difference (Fig. 1), we see that clusters with even n are much more stable than odd clusters.

The total oxygen binding energy is defined as:

$$\Delta E_n = E(Ce_6O_n) - E(Ce_6) - 1/2nE(O_2), \quad (2)$$

where $E(O_2)$ is the energy of O_2 molecule in gas phase, and the stepwise oxygen binding energy is then:

$$\Delta\Delta E = \Delta E_n - \Delta E_{n\text{-}1}, \quad (3)$$

and the average oxygen binding energy is $\Delta E = \Delta E_n/n$. From the stepwise oxygen binding energy (Fig. 1), we see that the binding of up to 12 oxygen atoms on the Ce_6 cluster is particularly thermodynamically favorable, and the average oxygen binding energy shows that binding of all 14 oxygen atoms to the Ce_6 cluster is still thermodynamically feasible. One can see that bare Ce_6O_8, Ce_6O_{10}, Ce_6O_{12} clusters have higher second energy difference values, indicating that these clusters are much more stable than their neighbors. Bare Ce_6O_8 has a closed-shell atomic structure of O_h symmetry with a hollow center. As a mater of fact, it is a fully symmetric fragment of the stable fluorite-type structure of bulk CeO_2. Such clusters may play an important role in crystallization of fluorite-like CeO_2 and defective fluorite-like (bixbyite-like) Ce_2O_3. There are several experimental reports on the synthesis of chemical compounds containing Ce_6O_8 fragments.[33,50,51]

Following the approach of Ref. 52, we evaluated the Gibbs free energy as:

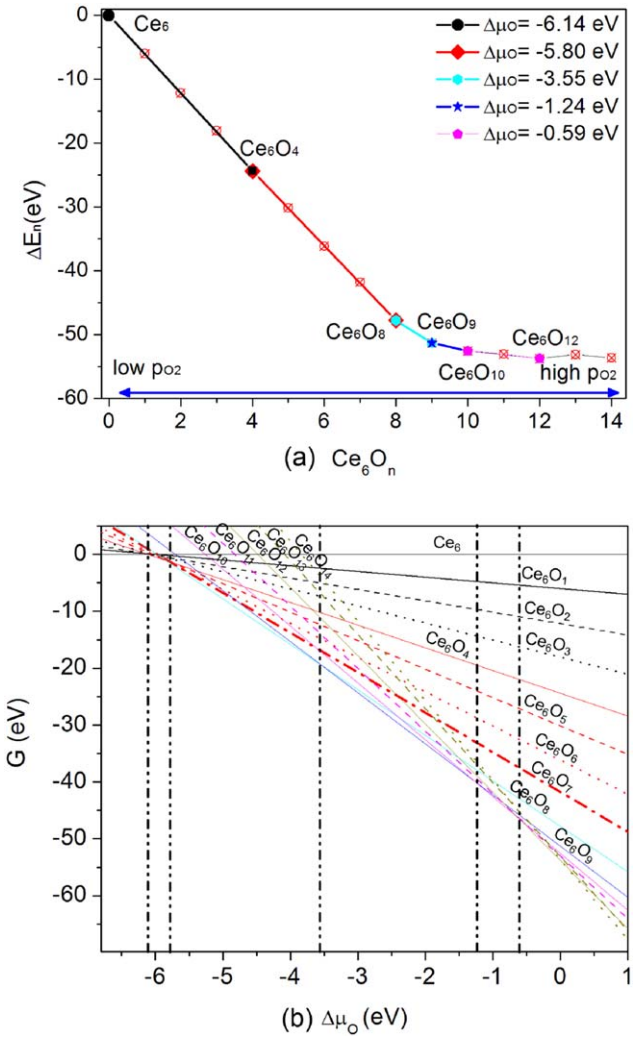

Figure 2. Phase diagram of Ce_6O_n ($n = 1$–14): stability of different clusters as a function of a) number of oxygen atoms and b) oxygen chemical potential.

$$\Delta G_f(T,\ P_{O2}) = F_{Ce6On}(T) - F_{Ce6}(T) - n\mu_O(T,p_{O2}), \quad (4)$$

where $F_{Ce6On}(T)$ and F_{Ce6} are the Helmholtz free energy of the Ce_6O_n and the pristine Ce_6 cluster (at their ground states with respect to the geometry and spin), respectively, and $\mu_O(T,p_{O2})$ is the chemical potential of oxygen. In equilibrium with molecular O_2 gas, $\mu_O(T,p_{O2})$ is expressed as:

$$\mu_O(T,p_{O2}) = 1/2\left[E_{O2} + \mu_{O2}(T,p^0) + k_BT\ln(p/p^0)\right], \quad (5)$$

where p^0, k_B, and p are the standard atmospheric pressure, Boltzmann constant, and oxygen partial pressure, respectively. E_{O2} was obtained by a spin-polarized calculation. $\mu_{O2}(T,p^0)$ term includes vibrational, rotational, and magnetic contributions for O_2 gas, and was taken from tables of thermodynamic data.[53] $k_BT\ln(p/p^0)$ is the contribution of temperature and O_2 partial pressure to the oxygen chemical potential. Figure 2a shows thermodynamics of bare Ce_6O_n clusters. There are six stable clusters: Ce_6, Ce_6O_4, Ce_6O_8, Ce_6O_9, Ce_6O_{10}, and Ce_6O_{12}. Another insightful form of the phase diagram is shown in Figure 2b. The phase diagram as a function of temperature and

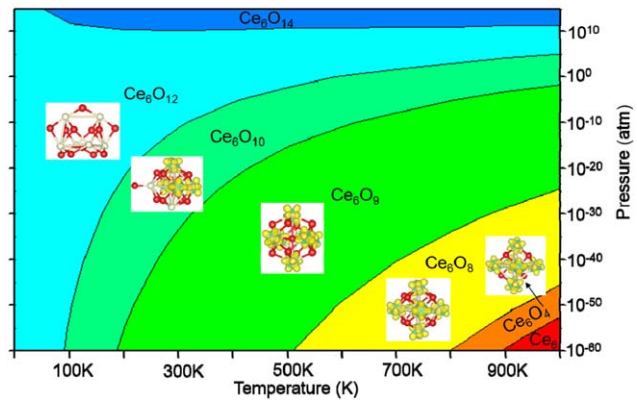

Figure 3. Phase diagram of Ce_6O_n in oxygen atmosphere. The spin density distribution (yellow) of the corresponding clusters is shown in the phase diagram.

partial oxygen pressure is shown in Figure 3. One can see that Ce_6O_8 has a wide stability field. Spin density distribution for Ce_6O_n clusters is also shown in Figure 3. Assuming that the oxidation state of O atom is −2, one can calculate that six Ce atoms in Ce_6O_{12} carry zero electrons, in Ce_6O_{10}—four electrons, in Ce_6O_9—six electrons, and in Ce_6O_8—eight electrons. It is noteworthy that Ce_6O_8 has six unpaired electrons (with one electron located on each Ce atom) and total magnetic moment of 6 μ_B. Remaining two electrons of Ce_6O_8 were found to participate in the formation of the 6c—2e σ bond, as will be further shown by the AdNDP analysis.

To understand the structure and bonding of the neutral Ce_6O_8 cluster, we performed a detailed MO analysis. Counting valence electrons, 6 Ce atoms give in total $6 \times 4 = 24$ electrons for bonding and 8 O atoms give in total 8×2 (O^{2-}) = 16 electrons. On balance, there are $24 - 16 = 8$ electrons. Understanding where these eight electrons localize or delocalize is very important for deciphering the stability of bare Ce_6O_8. Figure 4 shows the electron localization function (ELF). ELF[54] proved to be a useful tool for studying chemical bonding in clusters and molecules. It is interesting to find that there is a concentration of electron density in the empty center of the bare Ce_6O_8 cluster, as shown in Figures 4b–4d. This is reminiscent of the newly predicted anion-deficient compound Mg_3O_2,[55] which is stable at high pressures and also features a maximum of ELF in the center of empty Mg_6 octahedra, corresponding to an electron pair localized in the voids of the structure. Figure 5 shows the total and projected densities of states (DOS). One can see that the highest occupied molecular orbital (HOMO) levels are mainly composed of O-p and Ce-d_{z2}, and the lowest unoccupied molecular orbital (LUMO) is mainly composed of the Ce-d_{z2}, Ce-p, and O-p orbitals. From the projected DOS shown in Figures 5a and 5b, there is clear splitting between the d and f orbitals. In addition, the MOs with energies in the range of −5 to −2.4 eV (see Fig. 5) are made of strongly hybridized Ce-s, Ce-p, Ce-d, and Ce-f orbitals, together with O-p forming bonding MOs. The most interesting MOs with energies in the range from −2 to −1 eV are mainly composed of O-p and Ce-f_3 orbitals. Here, orbital Ce-f_3 is a coordinate-system-dependent symbol. The

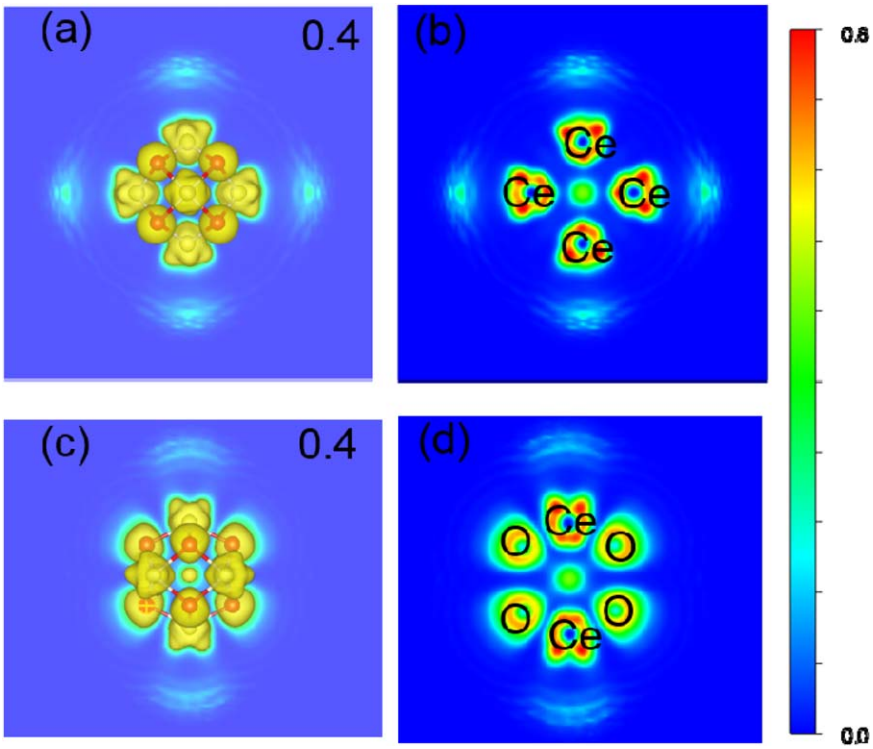

Figure 4. a) 3D and b) 2D images of the ELF of bare Ce_6O_8 cluster; c) 3D and d) 2D ELF of Ce_6O_8 cluster across the Ce-O-O-Ce-O-O plane. [Color figure can be viewed in the online issue, which is available at wileyonlinelibrary.com.]

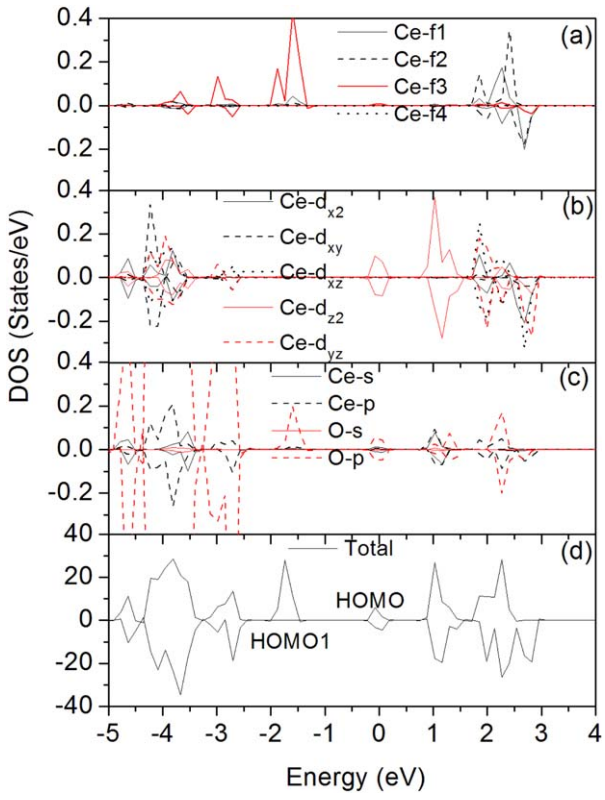

Figure 5. Total and projected DOS of the Ce_6O_8 cluster. [Color figure can be viewed in the online issue, which is available at wileyonlinelibrary.com.]

unpaired f_3 electrons contribute to the magnetic moment of Ce_6O_8, and there are six electrons responsible for the magnetic moment of Ce_6O_8 (6 μ_B). Another interesting bonding MO with energies between −0.5 and 0 eV is mainly composed of the O-p and Ce-d_{z2} orbitals. The six Ce atoms contribute two delocalized electrons as shown in the 3D and 2D partial charge plots (see Supporting Information Fig. S1). The antibonding states with energies from 0.0 to 0.5 eV are mainly due to the O-p and Ce-d_{z2} orbitals. The antibonding states in the energy range from 1 to 1.5 eV are made of O-p and Ce-p, Ce-d_{z2} orbitals.

To interpret the results obtained from ELF and DOS, we have further utilized the NBO method as well as its extension, the AdNDP algorithm. While NBO allows determination of Lewis elements of localized bonding, such as 1c—2e bonds (lone pairs [LP]) and 2c—2e bonds (classical two-center two-electron bonds), AdNDP enables delocalized bonding (*nc*—2e bonds, $n > 2$) to be found in addition. As bare Ce_6O_8 was shown to have six unpaired electrons, we used the unrestricted AdNDP (UAdNDP) analysis, which enables separate treatments of α- and β-valence electrons. To get an averaged result for a bond, we added these numbers together for the same type of bonds found by the program. In total, there are 39 α- and 33 β-valence electrons in the bare Ce_6O_8 cluster. The NBO method revealed the following chemical bonding elements: 8 α- and 8 β-electrons on eight oxygen atoms forming one LP on each oxygen with the total (α- and β-) occupation number (ON) ON = 1.8 |e| (Fig. 6a). It is noteworthy that these LPs are formed by the 2s AO's (56%) with the contribution of 2p AO's (44%) of oxygen. It also revealed six alpha-electrons of

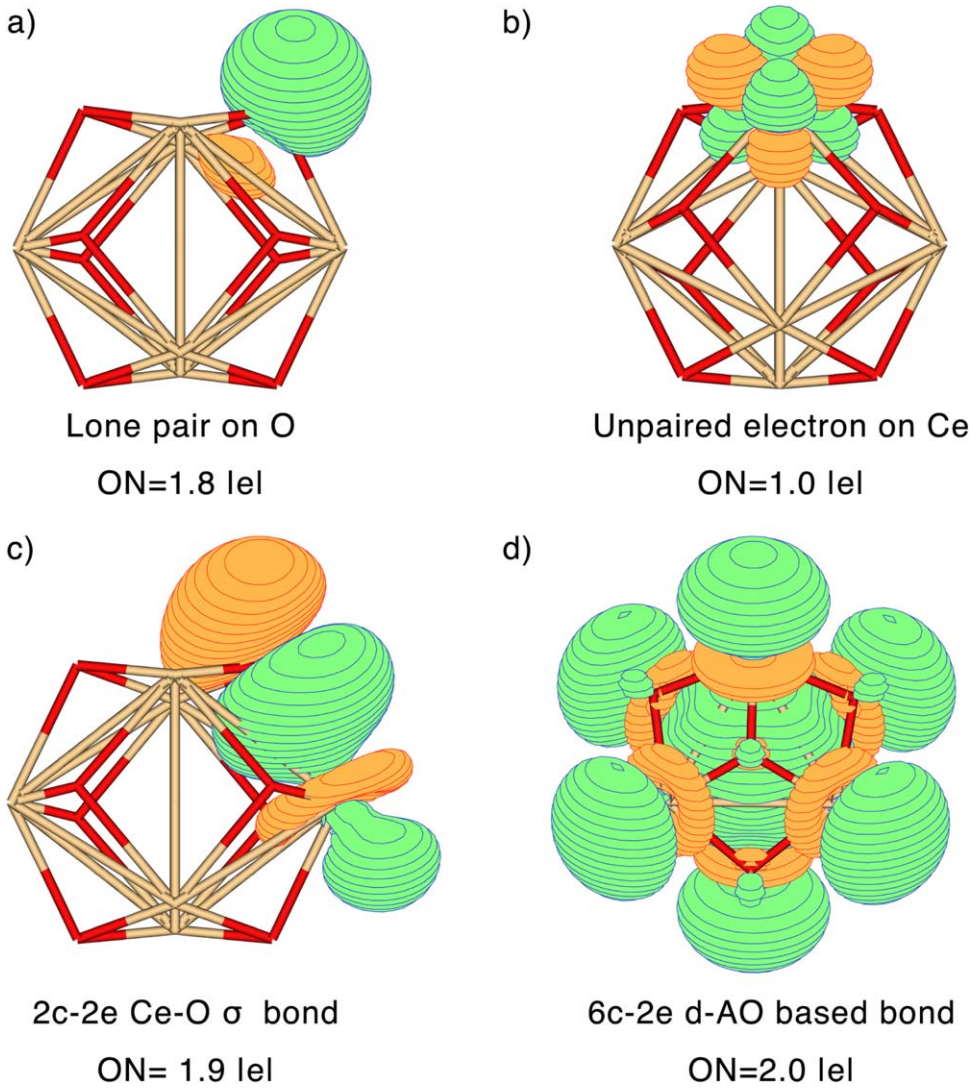

Figure 6. Representative elements of chemical bonding elements of the Ce_6O_8 cluster revealed by the NBO and AdNDP methods: a) LP on oxygen, b) unpaired electron on Ce, c) 2c—2e Ce—O σ bond, and d) 6c—2e d-AO-based σ bond. [Color figure can be viewed in the online issue, which is available at wileyonlinelibrary.com.]

f-type on 6 Ce atoms (one on each) with ON = 1.0 |e|, which make the cluster paramagnetic (Fig. 6b), in excellent agreement with the Ce-f_3 states observed in the projected DOS. According to the symmetry of the cluster, one could expect the formation of either 24 2c—2e Ce—O σ bonds or 24 LPs on oxygen atoms. However, the NBO analysis revealed a mixed picture with some Ce—O σ bonds (highly polarized toward oxygen: about 95% of the electron density comes from oxygen atoms and 5% from cerium atoms) and some LPs on oxygen breaking high symmetry of this cluster. That could be a result of the global and local orthogonality requirements in this method. Therefore, we searched for the 2c—2e Ce—O σ bonds using the UAdNDP method. The total UAdNDP picture (averaged for α- and β-electrons) revealed 24 2c—2e Ce—O σ bonds (ON = 1.9 |e|) highly polarized toward oxygen (Fig. 6c), which can also be obtained as LPs of oxygen atoms with ON = 1.7 |e| directed toward cerium atoms, which is in agreement with the overall NBO picture. All these bonding elements (6 unpaired electrons on 6 Ce atoms, 8 LPs on 8 O atoms, and 24 2c—2e Ce—O bonds) revealed by the NBO and UAdNDP methods account for a total of 70 electrons, whereas in total there are 72 electrons in the neutral Ce_6O_8 cluster. UAdNDP method enabled us to find the elements of delocalization (nc—2e bonds, $n > 2$) and helped to resolve this issue. UAdNDP has found one delocalized bond with ON = 2.0 |e|: 6c—2e σ bond of spherical shape spread over six cerium atoms (Fig. 6d), which is mostly composed of $5d_{z2}$ AO's of cerium atoms, thus making Ce_6O_8 cluster d-AO-based spherically σ aromatic. Thus, based on this chemical bonding picture one could assign the oxidation states of +2.67 to Ce atoms, and −2 to O atoms. Noteworthy, this kind of aromaticity is more related to the aromaticity of closo boranes (aromaticity due to "internal" or "cage" electrons) than that of negatively charged fullerenes (aromaticity due to "external" or "surface" electrons). To the best of our knowledge, this is the first example of spherical d-AO-based σ aromaticity.

The HOMO–LUMO energy separation serves as a simple approximate measure of chemical stability. Bare Ce_6O_8 cluster is found to possess a large HOMO–LUMO gap (0.9 eV). The high symmetry of neutral Ce_6O_8 cluster increases the DOS in the frontier orbital region: the HOMO-1 (a_{2g}), HOMO-2 (t_{2u}), and HOMO-3 (e_g) are essentially degenerate. As a matter of fact, these half-occupied MOs are transformed during the NBO procedure into six unpaired electrons of f-type found on six Ce atoms (one on each). Indeed, doubly occupied HOMO (a_{1g}) is responsible for the formation of the unique d-AO-based 6c—2e σ bond, making this cluster aromatic. The canonical MOs of the frontier orbitals are shown in Supporting Information Figure S2. Thus, spherical d-AO-based σ aromaticity in this cluster is a new mode of chemical bonding that can only occur in multinuclear transition metal and lanthanide oxide systems.

Conclusions

In conclusion, we have demonstrated a unique d-AO spherical σ-type aromaticity in a lanthanide oxide cluster, predicted by evolutionary structure prediction code USPEX and DFT + U calculations. Aromaticity and sphere-like geometry make the bare Ce_6O_8 cluster very stable, which is confirmed by the analysis of the thermodynamic properties. Thus, we believe that bare Ce_6O_8 may serve as a nucleation seed for many known complexes as well as a building block for CeO_2 and Ce_2O_3 crystals. The presence of $Ce^{2.67+}$ and a peculiar 6c—2e bond are likely to make this cluster and its derivatives very interesting for catalysis. Current findings suggest that d-AO-based σ aromaticity may exist in many spherical transition metal and lanthanide systems in low oxidation states. We hope that this work will inspire experimental realization of this and other transition metal and lanthanide oxides clusters possessing d-AO based spherical aromaticity.

Acknowledgments

The authors gratefully acknowledged the Division of Research Computing in the Office of Research and Graduate Studies at Utah State University for computer, storage, and other resources. This work is dedicated to the memory of Professor Paul von Ragué Schleyer.

Keywords: d-AO aromaticity · chemical bonding · Ce_6O_8 · evolutionary program · natural bond orbital analysis

How to cite this article: X. Yu, A. R. Oganov, I. A. Popov, A. I. Boldyrev *J. Comput. Chem.* **2015**, DOI: 10.1002/jcc.24049

Additional Supporting Information may be found in the online version of this article.

[1] I. A. Popov, A. I. Boldyrev, In The Chemical Bond: Chemical Bonding across the Periodic Table; G. Frenking; S. Shaik, Eds.; Wiley-VCH: Weinheim, **2014**; pp. 421—444.
[2] J. M. Mercero, A. I. Boldyrev, G. Merino, J. M. Ugalde, *Chem. Soc. Rev.* (in press), DOI:10.1039/c5cs00341e.
[3] W. N. Lipscomb, A. R. Pitochelli, M. F. Hawthorne, *J. Am. Chem. Soc.* **1959**, *81*, 5833.
[4] J. Aihara, *J. Am. Chem. Soc.* **1978**, *100*, 3339.
[5] R. B. King, D. H. Rouvray, *J. Am. Chem. Soc.* **1977**, *99*, 7834.
[6] H. W. Kroto, J. R. Heath, S. C. O'Brien, R. F. Curl, R. E. Smalley, *Nature* **1985**, *318*, 162.
[7] Z. Chen, J. I. Wu, C. Corminboeuf, J. Bohmann, X. Lu, A. Hirsch, P. v. R. Schleyer, *Phys. Chem. Chem. Phys.* **2012**, *14*, 14886.
[8] M. Garcia-Borras, S. Osuna, J. M. Luis, M. Swart, M. Solà, *Chem. Soc. Rev.* **2014**, *43*, 5089.
[9] A. Hirsch, Z. Chen, H. Jiao, *Angew. Chem. Int. Ed.* **2000**, *39*, 3915.
[10] A. Hirsch, Z. Chen, H. Jiao, *Angew. Chem. Int. Ed.* **2001**, *40*, 2834.
[11] J. Poater, M. Solà, *Chem. Commun.* **2011**, *47*, 11647.
[12] Z. Chen, R. B. King, *Chem. Rev.* **2005**, *105*, 3613.
[13] X. Li, H. F. Zhang, L. S. Wang, A. E. Kuznetsov, N. A. Cannon, A. I. Boldyrev, *Angew. Chem. Int. Ed.* **2001**, *40*, 1867.
[14] X. Li, A. E. Kuznetsov, H. F. Zhang, A. I. Boldyrev, L.-S. Wang, *Science* **2001**, *291*, 859.
[15] X. W. Li, W. T. Pennington, G. H. Robinson, *J. Am. Chem. Soc.* **1995**, *117*, 7578.
[16] X. W. Li, Y. Xie, P. R. Schreiner, K. D. Gripper, R. C. Crittendon, C. F. Campana, H. F. Schaefer, G. H. Robinson, *Organometallics* **1996**, *15*, 3798.
[17] B. Twamley, P. P. Power, *Angew. Chem. Int. Ed.* **2000**, *39*, 3500.
[18] R. J. Wright, M. Brynda, P. P. Power, *Angew. Chem. Int. Ed.* **2006**, *45*, 5953.
[19] A. E. Kuznetsov, A. I. Boldyrev, H. J. Zhai, X. Li, L. S. Wang, *J. Am. Chem. Soc.* **2002**, *124*, 11791.
[20] J. Li, C. W. Liu, J. X. Lu, *J. Cluster Sci.* **1996**, *7*, 469.
[21] J. Li, C. W. Liu, J. X. Lu, *Polyhedron* **1994**, *13*, 1841.
[22] J. Li, C. W. Liu, J. X. Lu, *J. Chem. Soc. Faraday Trans.* **1994**, *90*, 39.
[23] J. Li, C. W. Liu, J. X. Lu, *J. Cluster Sci.* **1994**, *5*, 505.
[24] X. Yang, T. Waters, X. B. Wang, R. A. J. O'Hair, A. G. Wedd, J. Li, D. A. Dixon, L. S. Wang, *J. Phys. Chem. A* **2004**, *108*, 10089.
[25] J. Li, *J. Cluster Sci.* **2002**, *13*, 137.
[26] X. Huang, H. J. Zhai, B. Kiran, L. S. Wang, *Angew. Chem. Int. Ed.* **2005**, *44*, 7251.
[27] H. J. Zhai, B. B. Averkiev, D. Y. Zubarev, L. S. Wang, A. I. Boldyrev, *Angew. Chem. Int. Ed.* **2007**, *46*, 4277.
[28] J. Zhang, A. N. Alexandrova, *J. Phys. Chem. Lett.* **2012**, *3*, 751.
[29] X. Zhang, G. Liu, G. Ganteför, K. H. Bowen, A. N. Alexandrova, *J. Phys. Chem. Lett.* **2014**, *5*, 1596.
[30] A. Nandula, Q. T. Trinh, M. Saeys, A. N. Alexandrova, *Angew. Chem. Int. Ed.* **2015**, *54*, 5312.
[31] A. J. Karttunen, M. Linnolahti, T. A. Pakkanen, P. Pyykko, *Chem. Commun.* **2008**, 465.
[32] P. Cui, H. S. Hu, B. Zhao, J. T. Miller, P. Cheng, J. Li, *Nat. Commun.* **2015**, *6*, 6331.
[33] R. Das, R. Sarma, J. B. Baruah, *Inorg. Chem. Commun.* **2010**, *13*, 793.
[34] A. R. Oganov, C. W. Glass, *J. Chem. Phys.* **2006**, *124*, 244704.
[35] A. R. Oganov, A. O. Lyakhov, M. Valle, *Acc. Chem. Res.* **2011**, *44*, 227.
[36] A. O. Lyakhov, A. R. Oganov, H. T. Stokes, Q. Zhu, *Comput. Phys. Commun.* **2013**, *184*, 1172.
[37] W. Zhang, A. R. Oganov, A. F. Goncharov, Q. Zhu, S. E. Boulfelfel, A. O. Lyakhov, E. Stavrou, M. Somayazulu, V. B. Prakapenka, Z. Konôpková, *Science* **2013**, *342*, 1502.
[38] Q. Zhu, D. Y. Jung, A. R. Oganov, C. W. Glass, C. Gatti, A. O. Lyakhov, *Nat. Chem.* **2013**, *5*, 61.
[39] G. Kresse, D. Joubert, *Phys. Rev. B* **1999**, *59*, 1758.
[40] G. Kresse, J. Furthmüller, *Phys. Rev. B* **1996**, *54*, 11169.
[41] J. P. Perdew, K. Burke, M. Ernzerh, *Phys. Rev. Lett.* **1996**, *77*, 3865.
[42] S. F. Li, H. Lu, P. Li, Z. Yang, Z. X. Guo, *J. Chem. Phys.* **2008**, *128*, 164718.
[43] C. W. M. Castleton, J. Kullgren, K. Hermansson, *J. Chem. Phys.* **2007**, *127*, 244704.
[44] E. D. Glendening, C. R. Landis, F. Weinhold, *Wiley Interdiscip. Rev. Comput. Mol. Sci.* **2012**, *2*, 1.
[45] D. Y. Zubarev, A. I. Boldyrev, *Phys. Chem. Chem. Phys.* **2008**, *10*, 5207.
[46] T. J. Gish, I. A. Popov, A. I. Boldyrev, *Chem. Eur. J.* **2015**, *21*, 5307.
[47] I. A. Popov, V. F. Popov, K. V. Bozhenko, I. Černušàk, A. I. Boldyrev, *J. Chem. Phys.* **2013**, *139*, 114307.
[48] L. M. Yang, I. A. Popov, A. I. Boldyrev, T. Heine, T. Frauenheim, E. Ganz, *Phys. Chem. Chem. Phys.* **2015**, *17*, 17545.
[49] (a) I. A. Popov, B. B. Averkiev, A. A. Starikova, A. I. Boldyrev, R. M. Minyaev, V. I. Minkin, *Angew. Chem. Int. Ed.* **2015**, *54*, 1476; *Angew. Chem. Int. Ed.* **2015**, *127*, 1496.

[50] C. Hennig, A. Ikeda-Ohno, W. Kraus, S. Weiss, P. Pattison, H. Emerich, P. M. Abdala, A. C. Scheinost, *Inorg. Chem*. **2013**, *52*, 11734.
[51] V. Mereacre, A. M. Ako, M. N. Akhtar, A. Lindemann, C. E. Anson, A. K. Powell, *Helv. Chim. Acta* **2009**, *92*, 2507.
[52] S. Bhattacharya, S. V. Levchenko, L. M. Ghiringhelli, M. Scheffler, *Phys. Rev. Lett*. **2013**, *111*, 135501.
[53] D. R. Stull, H. Prophet, JANAF thermochemical tables, 2nd.; U.S. National Bureau of Standards: U. S. EPO, Washington D. C., DTIC Document, **1971**.
[54] B. Silvi, A. Savin, *Nature* **1994**, *371*, 683.
[55] Q. Zhu, A. R. Oganov, A. O. Lyakhov, *Phys. Chem. Chem. Phys*. **2013**, *15*, 7696.

Received: 24 May 2015
Revised: 22 July 2015
Accepted: 23 July 2015
Published online on 00 Month 2015